The ZIMPOL high contrast imaging polarimeter for SPHERE: design, manufacturing and testing

Ronald Roelfsema[a], Hans Martin Schmid[b], Johan Pragt[a], Daniel Gisler[b], Rens Waters[j] , Andreas Bazzon[b], Andrea Baruffolo[c], Jean-Luc Beuzit[d], Anthony Boccaletti[e], Julien Charton[d], Claudio Cumani[f], Kjetil Dohlen[g], Mark Downing[f], Eddy Elswijk[a], Markus Feldt[h], Charlotte Groothuis[a], Menno de Haan[a], Hiddo Hanenburg[a], Norbert Hubin[f], Franco Joos[b], Markus Kasper[f], Christoph Keller[i], Jan Kragt[a], Jean-Louis Lizon[f], David Mouillet[d], Alexey Pavlov[h], Florence Rigal[a], Sylvain Rochat[d], Bernardo Salasnich[c], Peter Steiner[b], Christian Thalmann[b,h], Lars Venema[a], Francois Wildi[k]

[a]NOVA-ASTRON, Oude Hoogeveensedijk 4, 7991 PD Dwingeloo, The Netherlands;
[b]Institute of Astronomy, ETH Zurich, 8093 Zurich, Switzerland;
[c]INAF, Osservatorio Astronomico di Padova, 35122 Padova, Italy;
[d]LAOG, BP 53X, 38041 Grenoble cedex 9, France;
[e]LESIA, Observatoire de Paris, 5 place J. Janssen, 92195 Meudon, France;
[f]ESO, Karl-Schwarzschild-Strasse 2, D-85748 Garching bei München, Germany
[g]LAM, UMR6110, CNRS/Universite de Provence, 13388 Marseille cedex 13, France;
[h]Max-Planck-Institut fur Astronomie, Königstuhl 17, 69117 Heidelberg, Germany;
[i]Sterrekundig Instituut Utrecht, Princetonplein 5, 3584 CC Utrecht, The Netherlands;
[j]Astronomical Institute "Anton Pannekoek", 1098 SJ Amsterdam, The Netherlands;
[k]Observatoire Astronomique de l'Universite de Geneve, 1290 Sauverny, Switzerland

ABSTRACT

ZIMPOL is the high contrast imaging polarimeter subsystem of the ESO SPHERE instrument. ZIMPOL is dedicated to detect the very faint reflected and hence polarized visible light from extrasolar planets. ZIMPOL is located behind an extreme AO system (SAXO) and a stellar coronagraph. SPHERE is foreseen to have first light at the VLT at the end of 2011. ZIMPOL is currently in the manufacturing, integration and testing phase. We describe the optical, polarimetric, mechanical, thermal and electronic design as well as the design trade offs. Specifically emphasized is the optical quality of the key performance component: the Ferro-electric Liquid Crystal polarization modulator (FLC). Furthermore, we describe the ZIMPOL test setup and the first test results on the achieved polarimetric sensitivity and accuracy. These results will give first indications for the expected overall high contrast system performance. SPHERE is an instrument designed and built by a consortium consisting of LAOG, MPIA, LAM, LESIA, Fizeau, INAF, Observatoire de Genève, ETH, NOVA, ONERA and ASTRON in collaboration with ESO.

Keywords: Extra-solar planets, imaging, polarimetry, high-contrast

1. INTRODUCTION

1.1 ZIMPOL science case

SPHERE-ZIMPOL[1,2,3] (Spectro-Polarimetric High Contrast Exoplanet Research - Zurich Imaging Polarimeter) is one of the first instruments which aim for the direct detection of reflected light from extra-solar planets. The instrument will search for direct light from old planets with orbital periods of several months to several years as we know them from our solar system. These are planets which are in or close to the habitable zone.

The reflected radiation is generally polarized and the degree of polarization may be particularly high at short wavelengths < 1μm due to Rayleigh scattering by molecules and scattering by haze particles in planetary atmospheres[4, 5]. For this reason the visual-red spectral region is well suited for planet polarimetry.

Therefore SPHERE-ZIMPOL will be capable to investigate only the very nearest stars for the polarization signal from extra-solar planets. There are half a dozen of good candidate systems for which giant planets should be detectable, even if their properties are not ideal (low albedo, not highly polarized). In another handful targets there is some chance to find high-polarization planets, if they exist around them. For stars further away a detection of reflected light with SPHERE-ZIMPOL will be difficult.

The search for reflected light from extra-solar planets is very demanding, because the signal decreases rapidly ($\sim 1/a^2$) with the orbital separation a. For a Jupiter-sized object and a separation of 1 AU the planet/star contrast to be achieved is on the order 10^{-8} for a successful detection. This is much more demanding than the direct imaging of young self-luminous planets.

Because the degree of polarization of a planet is measured relative to the local background light (from the central star), it can in principle be obtained with very high accuracy without the need for an absolute instrument calibration.

The ZIMPOL high precision imaging polarimetry will certainly be very powerful for the investigation of the scattering polarization from circumstellar disks and dust shells around bright young and evolved stars. ZIMPOL can also be used in non-polarimetric mode for coronagraphic and non-coronagraphic high contrast imaging in the 550 – 900 nm range for the investigation of the circumstellar regions around stars bright enough for wave front sensing (about R<10 mag). The system will provide a diffraction limited resolution of 16 mas in the R-band with an AO Strehl ratio of up to 50%.

1.2 SPHERE-ZIMPOL outline

ZIMPOL is one of the four sub-systems of SPHERE[6] (figure 1). The design of SPHERE is divided into four subsystems: the Common Path and Infrastructure (CPI) and the three science channels: a differential imaging camera (IRDIS[7], Infrared Dual Imager and Spectrograph), an Integral Field Spectrograph (IFS[8]), and a visible imaging polarimeter (ZIMPOL). The Common Path includes pupil stabilizing fore optics (tip-tilt and derotator) where insertable polarimetric half-wave plates are also provided, the SAXO extreme adaptive optics system with a visible wavefront sensor, and NIR and Vis coronagraphic devices. ZIMPOL shares the visible channel with the wavefront sensor.

The instrument will be mounted to the Nasmyth platform rather than directly attached to the telescope Nasmyth rotator which is not adapted to carry the full charge of the instrument bench. All the sub-systems will be mounted onto a bench which is actively damped by a pneumatic servo-controlled system and equipped with a dust cover.

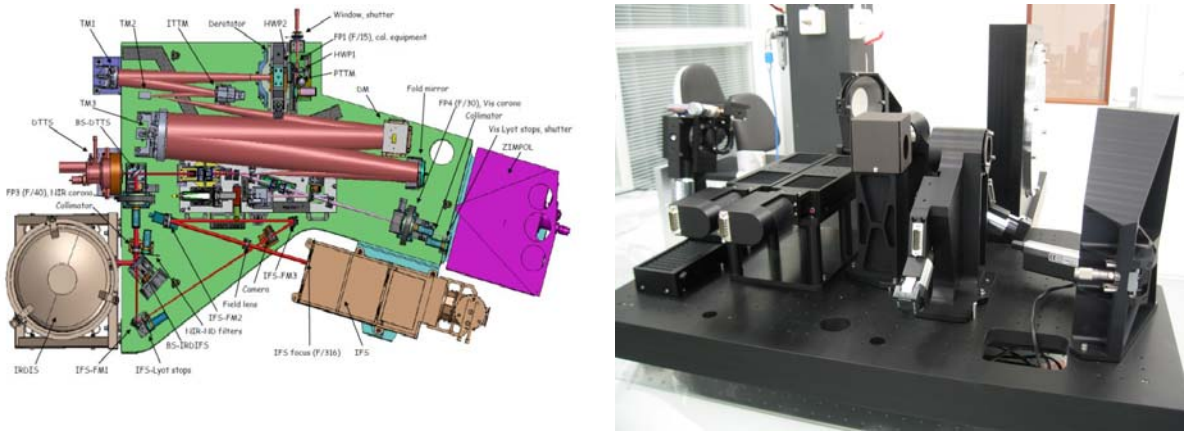

Figure 1. Left) SPHERE optical bench with the location of the ZIMPOL sub-system shown in purple. (Right) The ZIMPOL bench during alignment

Among ZIMPOL's main specifications are a bandwidth of 600 to 900 nm (with a goal of 500 to 900 nm) and an instantaneous field of view of 3 x 3 arcsec2 with access to a total field of view of 8 arcsec diameter by an internal field selection mechanism. The ZIMPOL optical train contains a common optical path that is split with the aid of a polarizing beamsplitter in two optical arms. Each arm has its own detector. The common path contains common components for both arms like calibration components, common filters, a switchable half wave plate and a Ferro Electric Liquid (FLC)

crystal polarization modulator. The two arms have the ability to measure simultaneously the two complementary polarization states in the same or in distinct filters. The images on both ZIMPOL detectors are Nyquist sampled at 600 nm. The detectors are both located in the same cryostat and cooled to -80 ^{o}C. The rest of the ZIMPOL opto-mechanical system is at ambient temperature.

ZIMPOL can be used in three polarimetric modes as well as in a classical imaging mode.

1.3 ZIMPOL specifications

ZIMPOL shall provide a very accurate relative linear polarization measurement for a localized signal within an image thanks to the simultaneous imaging of opposite polarization states (e.g. I_0 and I_{90}) with a fast polarimetric modulation – demodulation technique.

This observation mode shall make possible to achieve a contrast of 10^{-8} in 4 hr (goal 3×10^{-9} in 15 hr) for a 30% polarized planet at 1" from a I=2.5 mag star with SNR=5.

Spectral range	600 – 900 nm (goal 500 – 900 nm)
Field of View (instantaneous)	3 x 3 arcsec^2
Field of View (total)	8 arcsec diameter
Wave Front Error	< 75 nm (goal < 50 nm)
Transmission	> 0.25 (goal > 0.40)
Polarimetric Sensitivity	$< 10^{-5}$
Polarimetric Accuracy	$< 10^{-3}$
Polarimetric Efficiency	> 0.9
Instrument Polarization	< 0.01

2. ZIMPOL INSTRUMENTAL TECHNIQUES

2.1 SPHERE ZIMPOL block-diagram

A block-diagram of the SPHERE instrument design that focuses on the components relevant to ZIMPOL is shown in figure 2. The components causing strong instrumental polarization (thick arrows) are marked with a thick outline. The mirror M4 and the polarization compensator (pol. comp.) are used to counteract these effects.

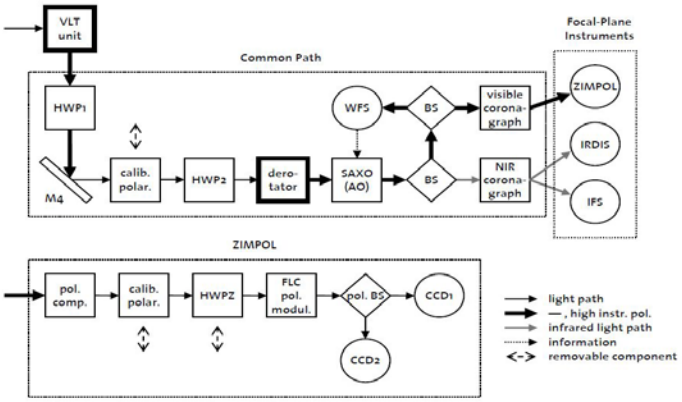

Figure 2. Block-diagram of SPHERE (top) and ZIMPOL (bottom) Abbreviations: BS = beam splitter, HWP = half-wave plate, WFS = wave-front sensor, FLC = ferro-electric liquid crystal..

2.2 Single difference: FLC & Detector

The basic ZIMPOL principle[9,10] (see figure 3) for high-precision polarization measurements includes a fast polarization modulator with a modulation frequency in the kHz range, combined with an CCD detector which demodulates the intensity signal in synchronism with the polarization modulation. The polarization modulator and associated polarizer convert the degree-of-polarization signal into a fractional modulation of the intensity signal, which is then measured in a demodulating detector system by a differential intensity measurement between the two modulator states. Each active pixel measures both the high and the low states of the intensity modulation and dividing the differential signal by the average signal eliminates essentially all gain changes, notably changes of atmospheric transparency or electronic gain drifts.

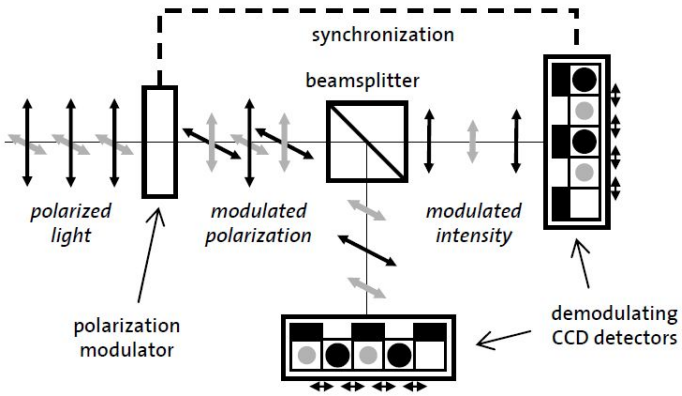

Figure 3. ZIMPOL operation principle

In ZIMPOL-SPHERE the modulator is a switchable half wave plate based on a Ferroelectric Liquid Crystal (FLC) element working at a frequency of about 1 kHz. The demodulator is a special ZIMPOL CCD camera which measures for each active pixel the intensity difference between the two modulation states. For this every second row of the CCD is masked so that charge packages created in the unmasked row during one half of the modulation cycle are shifted for the second half of the cycle to the next masked row, which is used as temporary buffer storage (the CCD is equipped with cylindrical micro-lenses which focus the light onto the open CCD rows). After many thousands of modulation periods the CCD is read out within less than one second. The sum of the two images is proportional to the intensity while the

normalized difference is the polarization degree of one Stokes component. Because the measurement is fully differential, systematic error sources are reduced to a very low level (on the order 10^{-5}). The main requirement is that the incoming signal is not strongly polarized ($p < 10^{-2}$).

2.3 Telescope polarization: M3 - HWP1 – M4

There are two main disturbing effects due to the telescope[11,12]. One is the polarization direction dependency on the zenith angle and the other is the wavelength dependent induced polarization.

At the VLT M3 is a folding mirror, which reflects the light coming from mirror M2 onto the Nasmyth platform towards the instruments. M3 has an incident angle of 45 degrees and has an aluminum coating. Thus M3 is responsible for strong polarization of the incoming light in the envisaged spectral range. In addition it rotates with time and changes therefore the induced polarization orientation.

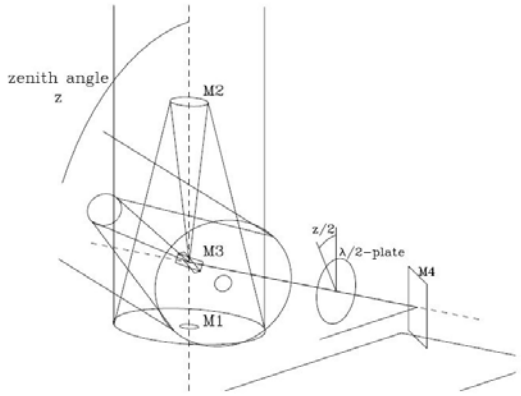

Figure 4. The M3-HWP1-M4 combination to reduce telescope polarization effects

The stabilization of the polarization direction is achieved by introducing a half-wave plate after M3. The half-wave plate (HWP1) is oriented in such a way, that its optical axis is at a position angle of half the zenith angle measured from vertical position (see figure 4). The half-wave plate flips the direction of the polarization introduced by M3 to a horizontal component (with respect to the Nasmyth platform). Regarding the instrument polarization, the combination of mirror M3 and rotatable half-wave plate HWP1 is equivalent to a mirror M3 being always in the same position, i.e. pointed towards zenith. In this way the two mirrors M3 (plus HWP1) and M4 act like two crossed mirrors so that the wavelength dependent telescope polarization introduced by M3 is cancelled by M4.

2.4 Double difference: Switching HWP2

By rotating a half-wave plate (HWP2) far upstream in the optical path by 45°, the sign of the incoming Stokes Q polarization is reversed. The instrumental aberrations, on the other hand, remain unchanged, resulting in the same background landscape as before. If the polarization images before and after the signal switching are subtracted from one another, the real polarization signals of the astronomical target add up constructively while the static background is canceled out. This method is only effective down to the level at which the background can be reproduced in the second image; any change to the optical path on the time scale of the signal switching (i.e. temporal differential aberrations) will lead to residual structures surviving in the double-difference image and will limit the detection of faint signals. The half-wave plate is foreseen to be switched about every 5 minutes during observation.

2.5 Derotator

The derotator causes strong polarization effects due to the large inclination angles[11]. For this reason only polarization position angles perpendicular and parallel to the orientation of the derotator will be transferred without strongly disturbing cross talk effect. Thus, the polarization directions to be measured have to be oriented, either parallel or

perpendicular to the derotator. One main purpose of HWP2 is to rotate the selected polarization into the "correct" orientation in order to pass more or less unaffected through the derotator.

2.6 Extreme Adaptive Optics: SAXO

SAXO[13] (SPHERE Adaptive optics for eXoplanet Observation) uses a deformable mirror of 180mm diameter with 41 × 41 actuators with inter-actuator stroke > ±3.5 μm, and a two-axis tip-tilt mirror with ±0.5mas resolution. Further downstream in the visible branch of the optical path, a Shack-Hartman wavefront sensor (WFS) with 40×40 lenslets operating in the 450 – 950 nm band at a temporal sampling frequency of 1.2 kHz using a 240 × 240 pixel electron-multiplying CCD detector feeds the corrective optics with real-time information, enabling a global AO loop delay below 1ms.

2.7 Coronagraph

The basic concept of the ZIMPOL coronagraph is a combination of a set of classical Lyot coronagraphs and 2 monochromatic Four Quadrant Phase Mask (4QPM) which provide a smaller inner working angle.

2.8 Shutter

ZIMPOL uses a frame transfer CCD. Therefore in principle a shutter is not required for ZIMPOL since a small level of light falling onto the detector during the frame transfer phase can be tolerated. However for ZIMPOL the frame transfer smearing becomes critical for the shortest exposure times (≈ 1sec) as foreseen for broad band filter observations of the brightest targets. For this reason a fast shutter which stops the light during the frame transfer phase (50 msec) is foreseen to improve the performance of the system.

2.9 Polarization compensator

The depth of the footprint of the reflected light from an exoplanet in the polarization image is typically on the order of 10^{-4} or less. It is embedded on a thick layer of background polarization of up to several 10^{-2}, caused by reflections on telescope mirrors and the polarization of the sky field. Since this background is quite flat over the field of view, it can be subtracted and therefore in itself poses no direct threat to planet detection. However, the effects of some noise sources like detector non-linearity or calibration errors scale in proportion with the background polarization level. Using software to subtract the flat polarization offset later at the data reduction stage does not undo these noise effects. They can only be avoided by removing the background polarization from the light before it reaches the polarimeter.

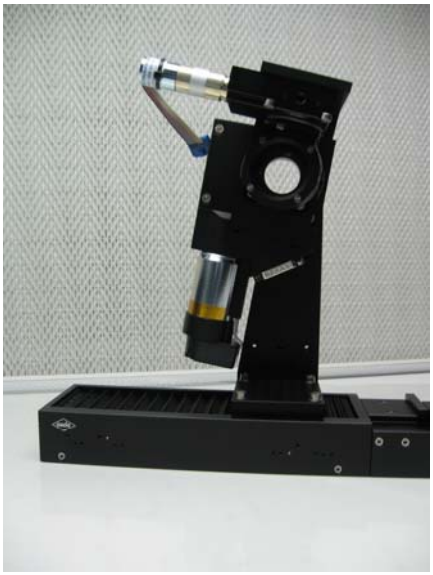

Figure 5. Implementation of the Polarization Compensator

The compensator is a very inexpensive but robust low-tech solution based on a simple uncoated glass plate[14] (see figure 5). Held into a light beam, the plate reflects a part of the incident light. If the incidence is not normal to the plate surface, the polarization component parallel to the tilt axis will preferentially be reflected. This polarized light is then "missing" from the transmitted light, leaving a polarization signature perpendicular to the tilt axis in the beam.

2.10 Dithering

Dithering is foreseen for all ZIMPOL observations to smooth fixed pattern noise on the detector and the effects of bad pixels. Dithering keeps the telescope pointed at a fixed position on the sky and the coronagraphic masks aligned while producing a series of movements of the tilt- and tip/tilt mirrors in front of the ZIMPOL cameras providing a series of x, y-shifts of the field of view by a certain number of pixels.

2.11 Double phase mode

A key property of the ZIMPOL concept is that each unmasked pixel of the detector records both of the two opposite polarization modes (I+ and I−). However, the pixel charges are shifted upwards and downwards within the CCD chip by the demodulation mechanism. The two photoelectron packages (corresponding to I+ and I−) created by a given CCD pixel are buffered in two different masked CCD pixels during their passive cycles (namely the pixels above and below the exposed pixel). The imperfections, traps or leaks that those buffer pixels as well as the charge shifting mechanism between them exhibit are not identical, and cause a fixed pattern noise in the resulting images, whose non-linear dependency on the local intensity and polarization makes it very resilient against corrective measures such as flat fielding, and which establishes a lower bound for the precision of the polarimeter.

A solution for these hardware noise effects is the two-phase observing mode[10]. Between two consecutive exposures, the demodulation phase is shifted by half a period, which means that the polarization component previously buffered in the rows above the exposed pixels is now buffered during the other half of the demodulation cycle in the rows below the exposed pixels, and vice versa. The two interlaced image series are summed up separately, so that the reduction software can undo the phase shift when calculating the polarization image.

Unfortunately, this method is rather sensitive to a background polarization. The traps and leaks of a CCD pixel depend on the number of charges stored and moved (i.e. the intensity in that particular image pixel). In case of a background polarization, the charges in the two component image pixels are not equal; therefore the hardware imperfections do not act identically on them, and a residue of the imperfection noise survives the reduction process into the polarization image, albeit at a much lower level than without the two-phase mode.

2.12 Angular Differential Imaging

Over the course of the observation, the VLT unit telescope's tracking will cause the observed sky field to rotate slowly with respect to the detector, whereas the optical elements responsible for aberrations will remain fixed in the instrument's frame of reference. This property can be exploited to discern the real signals originating in the sky from spurious instrumental effects through so-called angular differential imaging[14,15].

A median average of all exposures of the observation run is calculated and subtracted from each individual exposure, removing all static parts of the image. Since the planet moves across the field in an arc during the observation, it does not leave a strong footprint in the median background and therefore survives the background subtraction. The exposures are then rotated into the sky's frame of reference such that the planet signals coincide and add up constructively, whereas any residual background noise is averaged down.

In cases where the natural field rotation is insufficient (e.g. for a star near the celestial pole) or erratic (near the zenith), the image orientation on the detector can be artificially changed in discrete steps using the field derotator optics. This "active" field rotation extends the limited natural rotation arc to 2 pi. This is particularly beneficial in the center of the field, where the natural arc length is usually very small.

3. ZIMPOL INSTRUMENT DESCRIPTION

3.1 Optical design

The ZIMPOL optical train (see figure 6) contains a common optical path that is split with the aid of a polarizing beamsplitter in two optical arms. Each arm has its own detector. The common path contains common components for

both arms like calibration components, common filters, a switchable half wave plate and a ferro electric liquid crystal polarization modulator.

The camera lens consists of multiple elements. The first element is common for both ZIMPOL arms and is glued to the polarizing beamsplitter. This solution prevents external ghosts between the beamsplitter and the flat optical element in front of the beamsplitter. The second elements of the camera are located in each of the two ZIMPOL optical arms to facilitate independent alignment of both arms. All the parallel surfaces in the collimated beam are tilted in order to evacuate external ghosts.

The F-number at the detector is F/221. This corresponds to 3.5 milli-arcsec per 30 μm on the CCD. ZIMPOL uses a frame transfer CCD with an image area of about 30 x 30 mm.

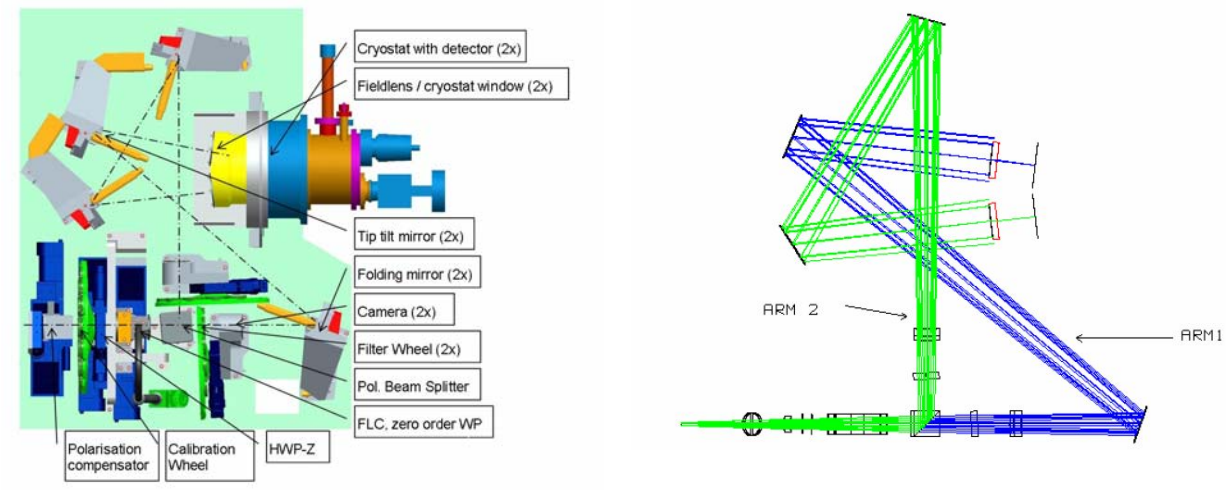

Figure 6. (Left) Description of ZIMPOL components on the optical bench, (Right) ZIMPOL optical design

The relative large F-number results in a relative long optical system. Compactness of the optomechanical system is ensured by adding folding mirrors in both ZIMPOL arms. The folding mirrors also locate the cryostat at the outside of the system in view of accessibility.

A total of 6 exposures are needed for 8 arcsec diameter image

Factor 1.1 over sampling compared to Nyquist criterion at 0.6 μm

Relative relaxed alignment requirements will allow a CPI-ZIMPOL alignment based on mechanical tolerances. Therefore during integration only optical alignment checks are foreseen but no optical adjustments.

Field lenses

The cryostat window acts as a field lens resulting in a telecentric system. A non telecentric beam will not focus on the correct pixels but rather on the masks at the side of the CCD. To overcome this problem a field lens in front of the micro-lenses is used in order to produce a telecentric beam. Drawbacks of this solution are extra curved optical elements and extra ghosts.

Zero Order Half Wave Plate

The wavelength dependence of a single FLC modulator is similar to a normal zero order wave plate; its retardance varies with wavelength roughly like 1/λ. In a combined design of a FLC modulator and a zero order half-wave plate it is possible to reduce the chromatic effects significantly. The achievable efficiency averaged over the range of 600 to 900 nm is about 93% for a single FLC modulator and about 99% when combined with a half-wave plate. A zero order plate

made of quartz will be used. It has a clear aperture of 24.5 mm and a thickness of 1.6 mm. To reduce optical surfaces the half wave plate will be placed on the exit window of the FLC modulator housing.

Blocking Filter

In order to achieve a very high contrast we must avoid out of band transmission leakage of the filters. This is in particular the case for coronagraphy where out of band wavelengths may not be blocked by the atmospheric dispersion corrector and coronagraph system. Therefore, a very strong signal from a dispersed central star has to be blocked in order to avoid a misinterpretation of the leakage as a faint, polarized planet signal. This is particularly harmful if the leaking signal has a different polarization than the in-band light so that it shows up in differential polarimetry. To reduce optical surfaces the blocking filter will be placed on the entrance window of the FLC modulator housing.

3.2 Mechanical design

ZIMPOL Optical Bench

The ZIMPOL Optical Bench will be mounted in a horizontal orientation on the CPI-Optical Bench. A major advantage for a horizontal ZIMPOL compared to a vertical implementation is reduced sensitivity to dust contamination. For a horizontal ZIMPOL the orientation of all critical optical surfaces is vertical. Vertical surfaces are about a factor of 10 less sensitive to dust accumulation than horizontal surfaces. The drawback of a horizontal implementation is reduced accessibility. Therefore ease of dismounting/remounting of critical components in view of maintenance and repairs have been key points for the mechanical design.

The ZIMPOL Optical Bench will be made of Aluminum (instead of Stainless Steel) in view of thermal conduction to balance thermal gradients. The opto-mechanical constructions are of aluminum with a black anodized coating.

All motors are standard of the shelf versions with a lifetime expected to be > 10 years for the expected duty cycle.

The whole opto-mechanical construction is inside a dust cover. During assembly or maintenance the instrument will be located in a cleanroom to keep the dust levels within the required limits.

Tip Tilt Mirrors

Tip-Tilt mirrors (TT) (see figure 7) are used for both dithering (small scale movements) and field selection (large scale movements). To facilitate similar operation of both ZIMPOL arms an equal length between TT-mirror and the detectors is used for both arms.

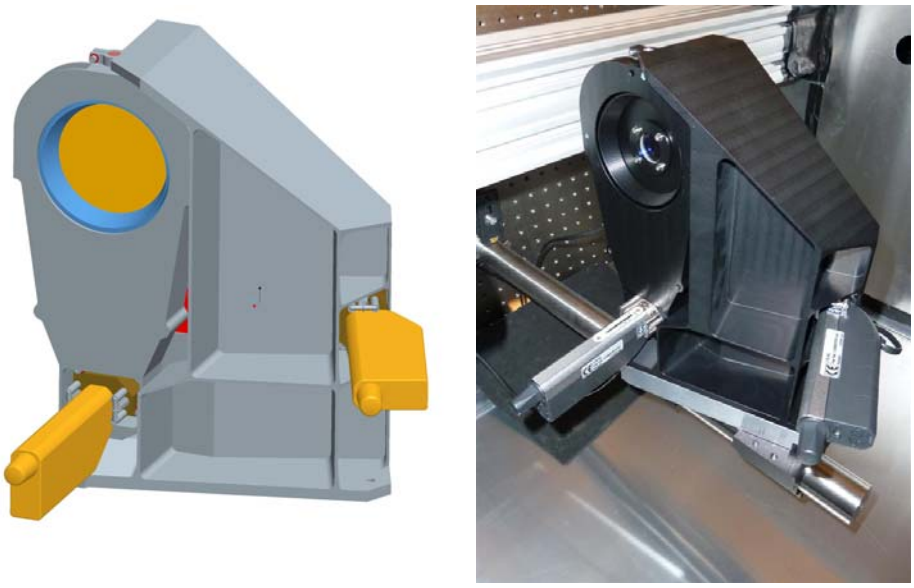

Figure 7. Motorized Tip-Tilt mirrors that are used for dithering and field selection

The distance between the CCD's in the cryostat is such that the field of view of one beam will never overlap the field of the other beam even for the extreme settings of the field selecting TT-mirrors. To avoid vignetting on the microlens-mask array directly in front of the ZIMPOL CCD's, the TT-mirrors will work in synchronization with preceding Tip mirrors.

3.3 Thermal and vacuum design

Detector Cryostat

The two ZIMPOL detectors will share a single ESO Standard Continuous Flow Cryostat (see figure 8). The cryostat is supplied with liquid Nitrogen from a standard 150 liters vessel that guarantees a typical hold time of 14 days. The use of only one cryostat reduces parts and overall mechanical and cryogenic complexity. Drawback is increased local optical and mechanical complexity to fit the two optical beams and both CCD's with additional electronics in a single detector head. Both CCD's will be mounted on a single baseplate. The alignment independence of the CCD's will be guaranteed by providing two sets of three shims for each CCD.

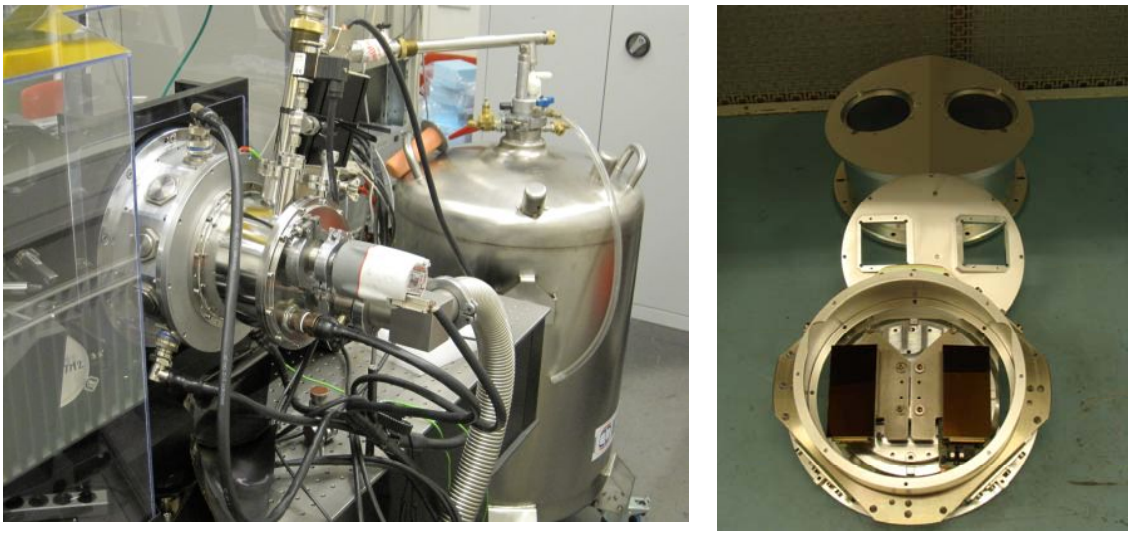

Figure 8. (Left) ESO Standard Continuous Flow Cryostat that houses both ZIMPOL CCDs. (Right) The two ZIMPOL CCDs and the field lenses that serve as cryostat windows with baffles in between.

To prevent damage to the fragile Micro Lens Array that is mounted on top of the ZIMPOL CCD's the cooldown speed of the Continuous Flow Cryostat is limited to < 0.5 K/min. The steady state operation temperature for the detectors is -80 ^{o}C.

FLC Vacuum Housing

The FLC must be heated to about 25 ^{o}C for optimal performance. In principle the ZIMPOL bench can be at 2 ºC during winter nights. To avoid image quality degradation due to turbulence induced by this temperature difference the FLC will be housed in a small vacuum vessel (see figure 9). This housing is equipped with temperature controllers to control the FLC temperature. Also a pressure sensor to monitor the vacuum is foreseen.

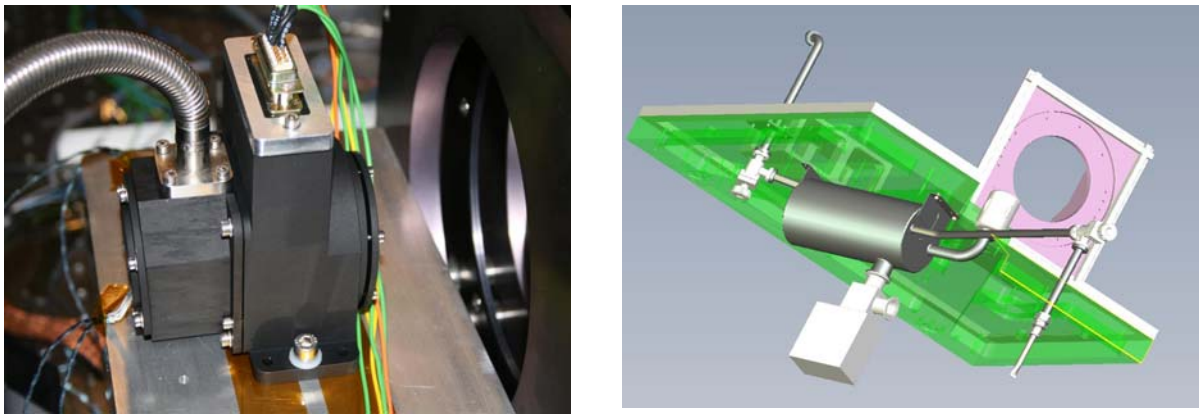

Figure 9. (Left) FLC modulator vacuum housing showing the warm FLC modulator in between the two cold windows. Window diameter is about 40 mm. (Right) FLC modulator vacuum buffer of 5 liter below the ZIMPOL Optical Bench and small getter pump to assure sufficient vacuum hold time for the FLC modulator housing.

The main requirement for the FLC housing is that the outside skin must not be warmer than 0.5 K than the direct environment. A thermal model shows that the heat conduction by air must be limited to 10 mW. For free molecular heat transfer of air this translates in a pressure requirement of the FLC vacuum chamber < 10-3 mbar.

During instrument operation the pumping system is switched off in view of vibrations. To maintain a vacuum level below 10e-3 mbar for the small volume of the FLC modulator vacuum housing, a 5 liter buffer volume that is located below the ZIMPOL bench is added. Also connected to the buffer volume is a small Barium getter pump (Alvatec ATG-3C). Based on a measured outgassing rate of 10e-7 Pam3/sec we expect a vacuum holdtime of about 50 days.

3.4 Detector System

CCD

To be suited for on-chip demodulation the ZIMPOL CCDs have to meet the following requirements:

Bidirectional vertical charge transfer (3-phase structure),

Frame transfer device

Very high vertical charge transfer efficiency (e.g. buried channel)

Fast vertical transfer (low image area electrode capacitance)

Low pixel to pixel cross talk

If the CCD is operated in half-frame (frame-transfer) mode, almost 100 % duty cycle, i.e. complete readout during integration can be achieved if the readout time is not longer than the integration time. CCD44-82bi from e2v technologies is an ideal choice for a large CCD. This CCD has a 3-phase architecture, and can be ordered as frame transfer CCD with an image area of 2k x 2k and a readout area of the same size. ZIMPOL charge shuffling requires a NIMO CCD type and this is also fulfilled by this device.

Micro Lens Array

The micro-lenses to be mounted on top of the CCD44-82 are structured as an array of cylindrical lenses onto the front side of a substrate. The aperture of the lenses d = 4 x 15µm = 60µm is corresponding to the vertical height of 4 pixel rows of the CCD. A very short focal length is advantageous for the optics. However there are restrictions of manufacturing and mechanical stability. A 525 µm substrate is the optimum of good optical properties and save manufacturing.

Opaque Strip Masks

To protect the storage rows of the CCD from light an opaque strip mask has to be structured on the backside of the micro-lens array (substrate). The required dimensions and alignment precision of the strip mask depend on the pixel to pixel cross talk of the CCD due to charge diffusion and light diffusion (scattering). The widths of opaque stripes are about 40 μm. Open areas of 20 μm are centered to the focal lines of the micro-lenses. The stripe mask will be produced as two absorbing CrOx layers and an opaque Cr layer on the substrate using micro-photolithographic methods.

Detector Control

ZIMPOL uses two e2v frame transfer CCD44-82 2kx4k Standard Silicon CCDs, one for each of the two polarization arms that are read out 2x2 binned (see figure 10). The CCD's are located in an ESO modified Double e2v Detector Head and Continuous Flow Cryostat (CFC). The detector controller NGC Detector Front End (DFE) consists of two basic boards mounted in a two-slot air cooled housing and standard NGC Power Supply with cable set to connect to the detector head. NGC provides the modulation clock and shutter control signals for the shutter/trigger. The shutter control signal is fed to the Shutter Driver. The modulation clock is fed to the FLC Modulation controller. NGC provides the reversing of the demodulation up and down shifts (up-down to down-up) in each second integration; i.e. it inverses the phase of the demodulation with respect to the modulation clocking. A custom FLC Modulation Controller (FLCMC) is used that provides the delay compensation (phase shifting) of the modulation clock, a backup solution to NGC reversing the demodulation up and down shifts, an on-off control signal to the GATE input of the FLC Driver and a guaranteed continuous DC free modulation signal for the times when NGC does not. The FLC Driver is a commercial Displaytec DR50 FLC Driver. For the shutter system a UniBlitz VCM-D1 Shutter Driver and normally open UniBlitz VS25 shutter are used. Cryo-vacuum control is done by an ESO standard Detector Vessel Controller called TeePee, based on the JUMO Imago 500 Multi-channel Process and Program Controller. The detectors system is controlled by an LLCU, NGC interface board and CCD-DCS software.

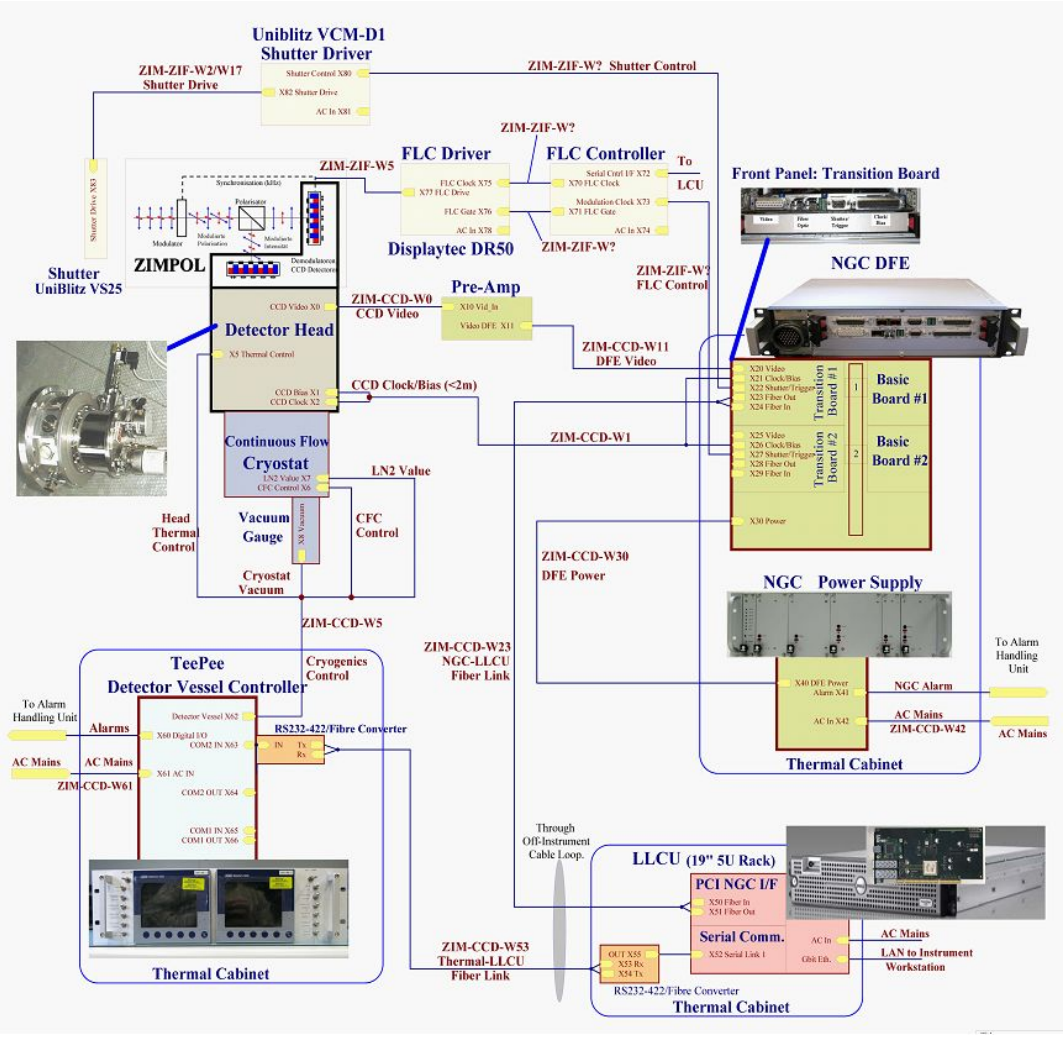

Figure 10. Schematic of the ZIMPOL detector control system

4. ZIMPOL TESTING

This section briefly describes the overall ZIMPOL sub-system tests that will take place at the premises of NOVA-ASTRON. The first part of the testing will be done with engineering CCD's. In a later stage (from July 2010) the science CCD's will be used.

The following test objectives are stated for the ZIMPOL sub-system testing: 1) Verify ZIMPOL Technical Specifications, 2) ZIMPOL sub system characterization and 3) Efficiency in preparation for SPHERE system level testing such that debugging has been done and Instrument Software (INS[16]) and Data Reduction Software (DRH[17]) is tested in an early stage in an environment much simpler than the complete SPHERE system.

At the present moment (June 2010) ZIMPOL testing is still at the functional level. Performance testing will start in July and continues until October. Delivery to LAOG for SPHERE system testing is foreseen for November 2010.

4.1 Test setup

The ZIMPOL test setup (see figure 11) contains the following optical components:

Sources: Star/planet simulator or an Iintegrating sphere as Flat Field lamp

Glass plate on motorized Tip-Tilt mechanism in diverging beam that provides real time fine alignment on the coronagraph based on feedback retrieved from the detector

Calibration unit that contains a linear polarizer, polarizer+QWP (circular polarizer) and QWP

Simple turbulence generator based on a rotating plate with some irregular layer (hairspray)

HWP2 mounted on a motorized rotation stage

Derotator mounted on a motorized rotation stage

Coronagraph: suspended round field mask with 5 λ/D diameter, round field mask with 3 λ/D diameter on a substrate and a 4QPM

Shutter

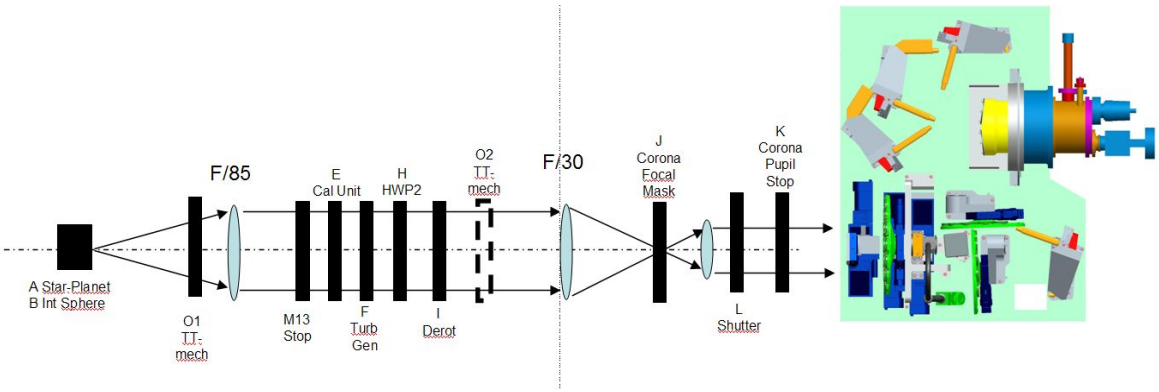

Figure 11. Schematic overview of the ZIMPOL optical test setup.

Simulating the detection of an exoplanet in the lab requires a small polarized signal on an extended unpolarized background. For this purpose a star-planet simulator (see figure 12) has been build based on the design from the University of Utrecht[18]. Source requirements are listed below:

Spectral range 500 – 900 nm

Star flux level sufficient for CCD full well < 0.5 sec

Star polarization level < 1 %

Star and planet must simulate point-source, i.e. source size < λ/D

Planet must be partially linearly polarized to about 30 %

The contrast ratio between star and planet must be set to fixed levels between 10-5 and 10-9

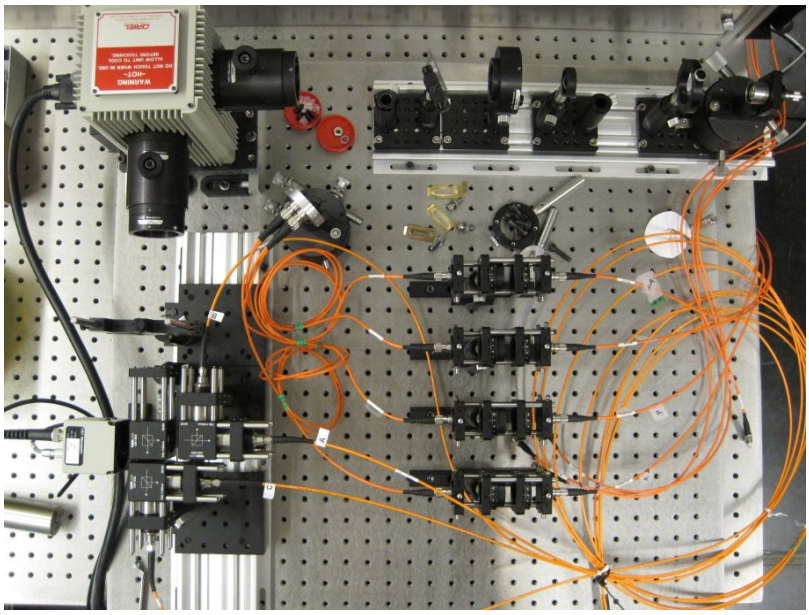

Figure 12 Hardware implementation of the star-planet simulator

4.2 First test results

FLC Differential Wave Front Error

The FLC-modulator is a key component in ZIMPOL. The ZIMPOL performance simulations[14, 15] showed that the differential aberrations introduced by the FLC modulator are critical for the ultimate performance of the instrument.

Specifications for the ZIMPOL FLC modulator are a phase differential aberration of 0.5 nm and a pointing differential aberration of 0.75 nm. With these properties it should be possible to reach with ZIMPOL the photon noise limit down to a contrast ratio of 10^{-8} (polarization flux of planet / flux of star).

The results as listed in figure 13 are obtained for the FLC modulator differential WFE. The figure gives the values that are used in the CAOS performance calculations for Standard Case4 (SC4). The figure also lists the measurement results that are obtained at the time of the PDR phase with a previous FLC. The last column of the figure lists the currently obtained measurement results with the improved FLC modulators FLC3 and FLC5.

FLC Dif. WFE results (nm)

	CAOS	PDR	FDR	FDR
	SC4	measured	FLC 3 measured	FLC 5 measured
phase	0.50	1.00	0.40	0.20
pointing	0.75	1.50	0.50	0.60
beamshift	0.75	1.50	0.50	0.50
RSS	**1.2**	**2.3**	**0.8**	**0.8**

Figure 13. Measurement results for the FLC differential Wave Front Error

It can be concluded from figure 13 that measured average values of the RMS differential WFE for FLC3 and 5 are within specifications.

Noise plot

The ZIMPOL sub-system is required to achieve photon limited polarimetric sensitivity down to the 10^{-5} . An engineering CCD has been used to obtain a plot of noise level versus photon flux (see figure 14). The theoretical photon noise is indicated with the solid line. Also the data of several test runs obtained under various test conditions are indicated. Clearly the system is reaching the detection goal of 10^{-5}.

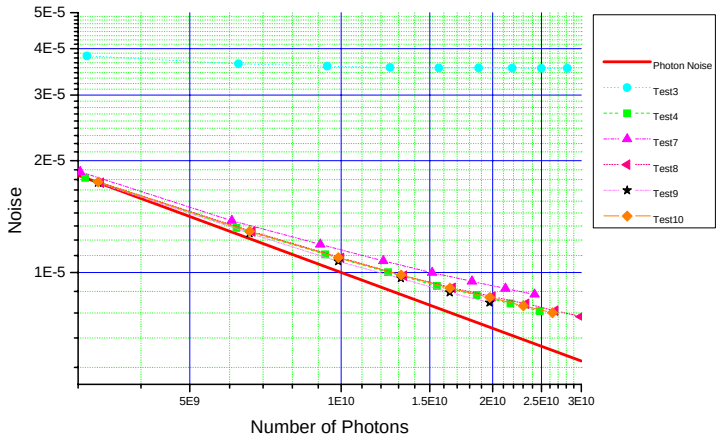

Figure 14. Noise level versus photon flux. The solid line indicates the theoretical photon noise limit.

Small signal in the field

Simulating the detection of an exoplanet in the lab requires a small polarized signal on an extended unpolarized background. A star-planet simulator and an engineering CCD have been used to detect two weak polarized point sources on a large background flux (see figure 15). The background noise level is about 8e-6. The signal strength of the strongest PSF is about 5 x10^{-5} and weakest PSF is about 3 x 10^{-5} . For the moment these result show that the test setup is ready to continue with extended and deeper performance tests.

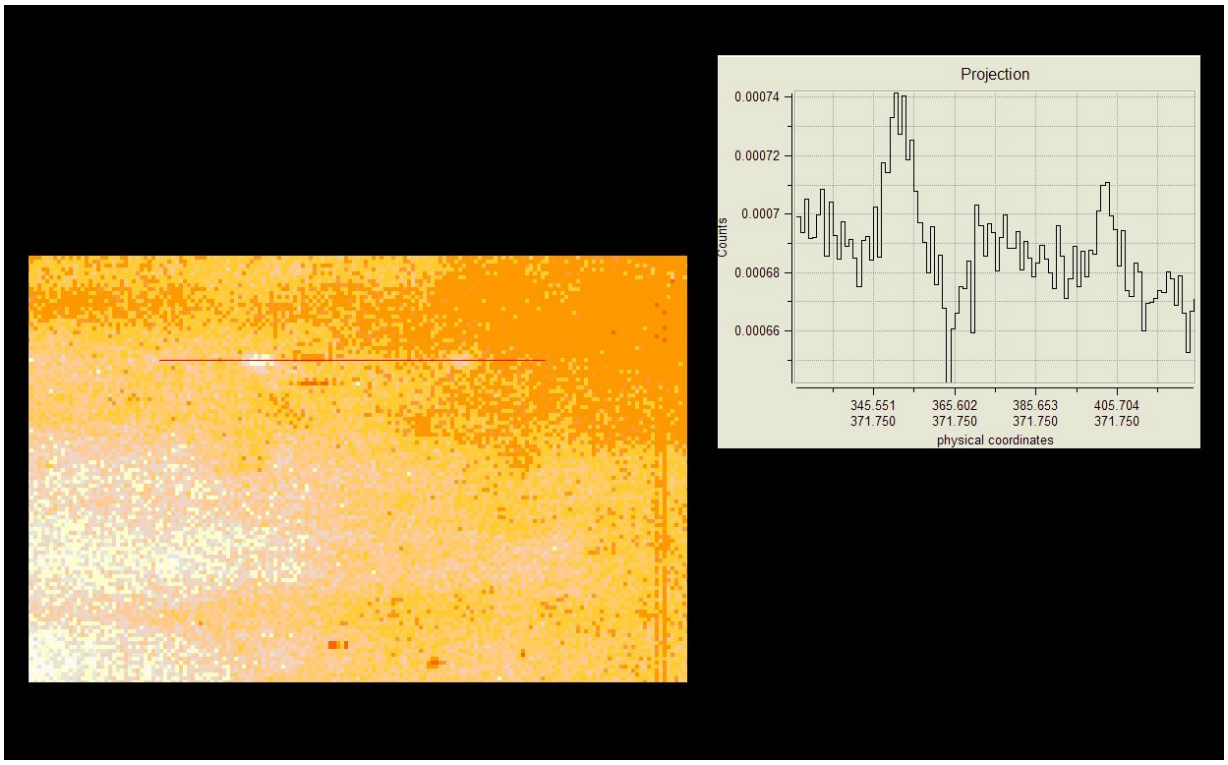

Figure 15. Detection of a weakly polarized signal on a large unpolarized background flux.

4.3 Coronagraph image

5. CONCLUSIONS AND OUTLOOK

We have described the SPHERE-ZIMPOL instrumental techniques, the instrument design and first test results.

Manufacturing, assembly and integration of the SPHERE-ZIMPOL subsystem will be finished early July 2010. An extensive test program will be followed between July and October to assess the ZIMPOL performance. ZIMPOL will be shipped to LAOG in November for integration with SPHERE. Overall system testing is foreseen for the first half year of 2011. The instrument will be shipped to Paranal in Q3 2011 for integration and commissioning at the VLT.

REFERENCES

[1] Schmid, H. M., Beuzit, J.-L., Feldt, M., Gisler, D., Gratton, R., Henning, T., Joos, F., Kasper, M., Lenzen, R., Mouillet, D., Moutou, C., Quirrenbach, A., Stam, D. M., Thalmann, C., Tinbergen, J., Verinaud, C., Waters, R., and Wolstencroft, R., “Search and investigation of extra-solar planets with polarimetry,” IAU Colloq. 200, 165–170 (2006)

[2] D. Gisler, H.M. Schmid, C. Thalmann, H.P. Povel, J.O. Stenflo, F. Joos, M. Feldt, R. Lenzen, J. Tinbergen, R. Gratton, R. Stuik, D.M. Stam, W. Brandner, S. Hippler, M. Turatto, R. Neuhäuser, C. Dominik, A. Hatzes, Th. Henning, J. Lima, A. Quirrenbach, L.B.F.M. Waters, G. Wuchterl, H. Zinnecker: Gisler CHEOPS/ZIMPOL: a VLT instrument study for the polarimetric search of scattered light from extrasolar planets. in: ``Ground-based instrumentation for astronomy'', A.F.M. Moorwood & M. Iye (eds.), SPIE Conf. Vol. 5492, 463-474 2004

[3] Beuzit, J.-L., Feldt, M., Dohlen, K., Mouillet, D., Puget, P., Antichi, J., Baruffolo, A., Baudoz, P., Berton, A., Boccaletti, A., Carbillet, M., Charton, J., Claudi, R., Downing, M., Feautrier, P., Fedrigo, E., Fusco, T., Gratton, R., Hubin, N., Kasper, M., Langlois, M., Moutou, C., Mugnier, L., Pragt, J., Rabou, P., Saisse, M., Schmid, H. M., Stadler, E., Turrato, M., Udry, S., Waters, R., and Wildi, F., "SPHERE: A 'Planet Finder' Instrument for the VLT," The Messenger 125, 29–34 (2006)
[4] D. M. Stam, Spectropolarimetric signatures of Earth-like extrasolar planets, A&A 482, 989-1007 (2008)
[5] E. Buenzli, H.M. Schmid: A grid of polarization models for Rayleigh scattering planetary atmospheres, Astron. Astrophys. 504, 259-276, 2009
[6] Jean-Luc Beuzit, Markus Feldt, Kjetil Dohlen, David Mouillet, Pascal Puget, François P. Wildi, Markus E. Kasper, And the SPHERE Consortium, SPHERE: a planet imager for the VLT, Proc. SPIE, Paper 7735-33 (2010)
[7] Kjetil Dohlen , Michel Saisse et al, Manufacturing and integration of the IRDIS dual imaging camera and spectrograph for SPHERE, Proc. SPIE, Paper 7735-102 (2010)
[8] Ricardo Claudi, SPHERE IFS: The spectro differential imager of the VLT for exoplanets search, Proc. SPIE, Paper 7735-179 (2010)
[9] Povel, H. P., Aebersold, F., and Stenflo, J., "Charge-coupled device image sensor as a demodulator in a 2-D polarimeter with a piezoelastic modulator," Appl. Opt. 29, 1186 (1990)
[10] Gisler, D., Instrumentierung fur hochprazise Vektorpolarimetrie in der Astronomie, PhD thesis, ETH Zurich (Switzerland) (2005)
[11] Joos, F., Polarimetry of Gas Planets, PhD thesis, ETH Zurich (Switzerland) (2007)
[12] Franco Joos, Esther Buenzli, Hans Martin Schmid and Christian Thalmann, Reduction of polarimetric data using Mueller calculus applied to Nasmyth instruments, Proc. of SPIE Vol. 7016, 70161I, (2008)
[13] J.-F. Sauvage, C. Petit, T. Fusco, T. Buey, A. Sevin, P. Bernardi, J. Charton, P. Feautrier, F. Wildi, K. Dohlen, J.-L. Beuzit, First laboratory results of the SPHERE eXtreme AO system: SAXO, Proc. SPIE, Paper 7736-14 (2010)
[14] Thalmann, C., Applications of High-Precision Polarimetry to Extrasolar Planet Search and Solar Physics, PhD thesis, ETH Zurich (Switzerland) (2008)
[15] Thalmann, Christian, Schmid, Hans M., Boccaletti, Anthony, Mouillet, David, Dohlen, Kjetil, Roelfsema, Ronald, Carbillet, Marcel, Gisler, Daniel, Beuzit, Jean-Luc, Feldt, Markus, Gratton, Raffaele, Joos, Franco, Keller, Christoph U., Kragt, Jan, Pragt, Johan H., Puget, Pascal, Rigal, Florence, Snik, Frans, Waters, Rens, Wildi, François, SPHERE ZIMPOL: overview and performance simulation, Proc. of SPIE Vol. 7014, 70143F, (2008)
[16] Baruffolo, P. Bruno, D. Fantinel, E. Fedrigo, L. Gluck, M. Kiekebusch, M. Micallef, B. Salasnich, P. Steiner, G. Zins, SPHERE Instrumentation Software in the Construction and Integration Phases, Proc. SPIE, Paper 7740-131 (2010)
[17] Ole Moeller-Nilsson, Markus Feldt, Aleksej I. Pavlov, SPHERE data reduction software: first insights into data reduction software development for next-generation instruments, Proc. SPIE, Paper 7740-76 (2010)
[18] N. Miesen, Master thesis, University Utrecht November 8, 2007